

H I Multibeam Survey Techniques

Lister Staveley-Smith

Australia Telescope National Facility, CSIRO,
PO Box 76, Epping, NSW 2121, Australia
lstavele@atnf.csiro.au

Received 1996 October 16, accepted 1996 December 12

Abstract: The parameters of the H I Parkes All-Sky Surveys (HIPASS), as proposed by the Multibeam Survey Working Group, are described, as are the advantages and disadvantages of various multibeam observing techniques, including telescope scanning. The best techniques, in terms of minimising the variance in image sensitivity, are calculated. Some of the observing techniques may be applicable to other multibeam surveys.

Keywords: instrumentation: detectors — techniques: image processing — surveys — radio lines: galaxies

1 Introduction

Although multi-element detectors are common in optical and IR astronomy, they are not yet commonly used in radio astronomy. This is partly because other techniques, such as synthesis interferometry, exist, and because of the technological difficulties in producing arrays that match the performance of highly optimised single-beam devices. Two notable differences exist between optical/IR and radio array detectors. The first is that the field of view of a typical radio telescope often does not allow a large number of detectors (Ruze 1965). The second is that, because of diffraction effects, it is extremely difficult to fill the focal plane and efficiently illuminate the aperture of a radio telescope simultaneously (Johansson 1995; Fisher 1997, present issue p. 96).

The Parkes 21 cm multibeam receiver (Staveley-Smith et al. 1996) is a conventional focal-plane array, with 13 beams arranged in a hexagonal grid. The spacing between adjacent beams is about two beamwidths, and therefore the array undersamples the focal plane. It is, however, optimised for efficient illumination and low system temperatures at 21 cm, and for the first time allows blind 21 cm surveys of very large areas of sky to be carried out.

Much of this volume is devoted to scientific issues relating to the new-generation surveys about to be made with the new Parkes 21 cm multibeam receiver. In this paper, I focus on the parameters of the two major extragalactic H I surveys proposed by the Multibeam Survey Working Group and give an overview of possible observing techniques that fill in the undersampled gaps either by dithering or scanning.

2 HIPASS

The scientific goals of the HIPASS and a technical description of the receiver have been outlined elsewhere (Staveley-Smith et al. 1996). The approximate parameters of the surveys, as envisaged by the Multibeam Survey Working Group, are given in Table 1 for reference. This table contains the expected parameters for the HIPASS, and an estimate of the theoretical detection limits. These detection limits will not be verified until the multibeam receiver is commissioned. The volume coverage is compared with previous and other continuing surveys by Schneider (1997, present issue p. 99). Other Parkes multibeam surveys, including a deep survey (see Disney & Banks 1997, present issue p. 69), are also proposed.

The first HIPASS, the Southern Sky Survey, is fairly shallow with an effective integration time of around 500 s for each beam area. Assuming that Nyquist sampling is desirable so that accurate positions can be obtained and extended structure can be faithfully reproduced, then about four pointings for each beam area are required. This implies a relatively short observing time for each point (125 s) and means that telescope control overheads will be very significant if the traditional point-and-shoot observing technique is used. Therefore a slow (active or drift) scan of the telescope across the sky, with continuous data collection, is probably the best observing technique for this survey (Sections 3.2 and 4).

The Zone of Avoidance survey is deeper, with an effective integration time of approximately 1800 s for each beam area; therefore, the choice of observing technique is not as constrained. At this

Table 1. Summary of the the expected parameters of the two major HIPASS

	Southern Sky Survey	Zone of Avoidance Survey
Sky coverage	$\delta \leq 0^\circ$	$\ell = 213^\circ$ to 33° , $ b \leq 5^\circ$
Integration time/beam	500 s	1800 s
Velocity coverage	-760 to 12200 km s^{-1}	-760 to 12200 km s^{-1}
Channel separation	13.2 km s^{-1}	13.2 km s^{-1}
Velocity resolution	16.0 km s^{-1}	16.0 km s^{-1}
Expected positional accuracy	$\leq 5'$	$\sim 5'$
Theoretical 5σ detection limit	20 mJy beam^{-1}	10 mJy beam^{-1}
Theoretical 5σ H I mass limit ($\Delta V = 200 \text{ km s}^{-1}$)	$10^6 d_{\text{Mpc}}^2 M_\odot$	$5 \times 10^5 d_{\text{Mpc}}^2 M_\odot$
Principal investigator	Webster	Staveley-Smith

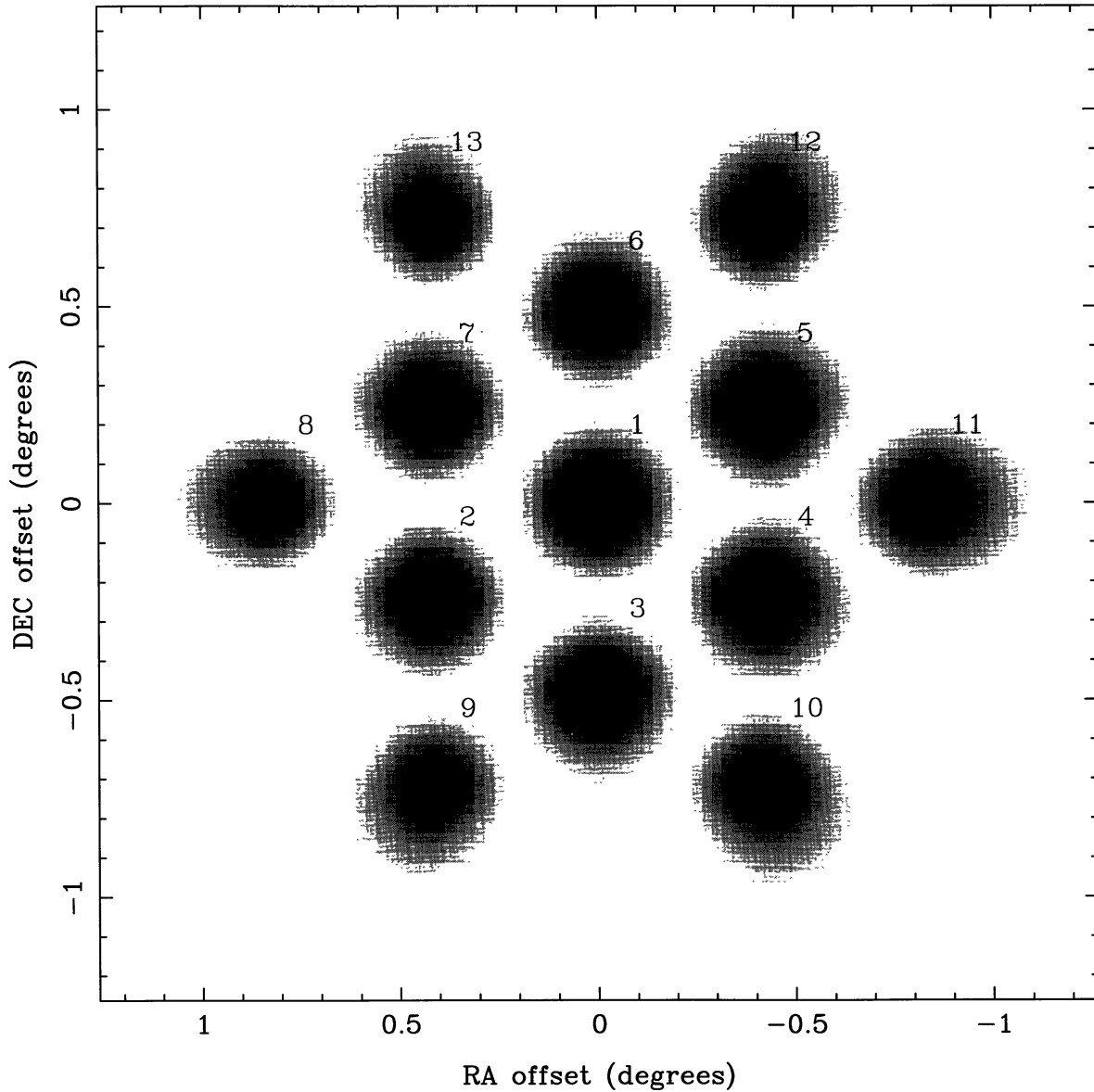


Figure 1—Theoretical beam sensitivity pattern for the Parkes multibeam instrument at 1370 MHz. The individual beam patterns (Trevor Bird, private communication) have a pixel size of $1.5'$ and have been added in quadrature to give this image. Intensity is inversely proportional to rms noise. Coma distortion (radial elongation of the beam patterns) is evident in the outer ring of six beams, although the beam efficiency is down by only 10%. The RA–DEC grid is appropriate for an observation on the northern meridian with the multibeam array at the nominal $pa = 0^\circ$. The principal electric field is in the vertical (DEC) direction.

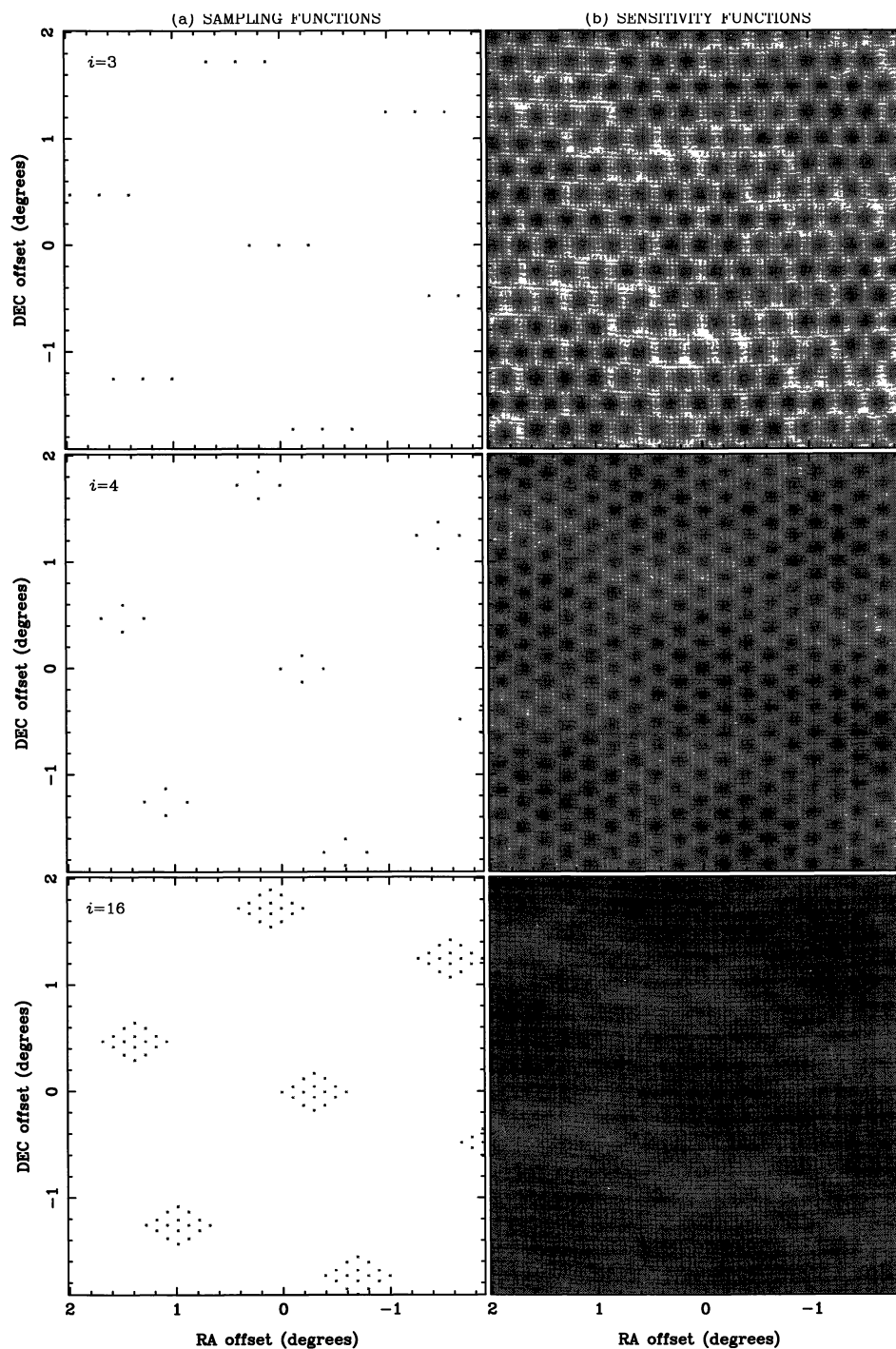


Figure 2—Three possible point-and-shoot sampling functions for the multibeam array on the left-hand side, with the corresponding sensitivity functions on the right-hand side. At top, $i = 3$ (see Table 2) fills in the largest gaps in the beam pattern, using three interleaved observations per field; $i = 4$ corresponds to a diamond-shaped interleave pattern giving a beam separation of $14'$; $i = 16$ corresponds to a nested diamond interleave with a $7'$ beam separation. Dark regions in the sensitivity functions have higher than average sensitivity.

stage (prior to commissioning), it is expected that a point-and-shoot technique (Section 3.1) will be used, in order to accommodate a piggyback Galactic

Plane pulsar survey. For sky-subtraction purposes, the telescope position will be frequently switched between adjacent fields (Section 4).

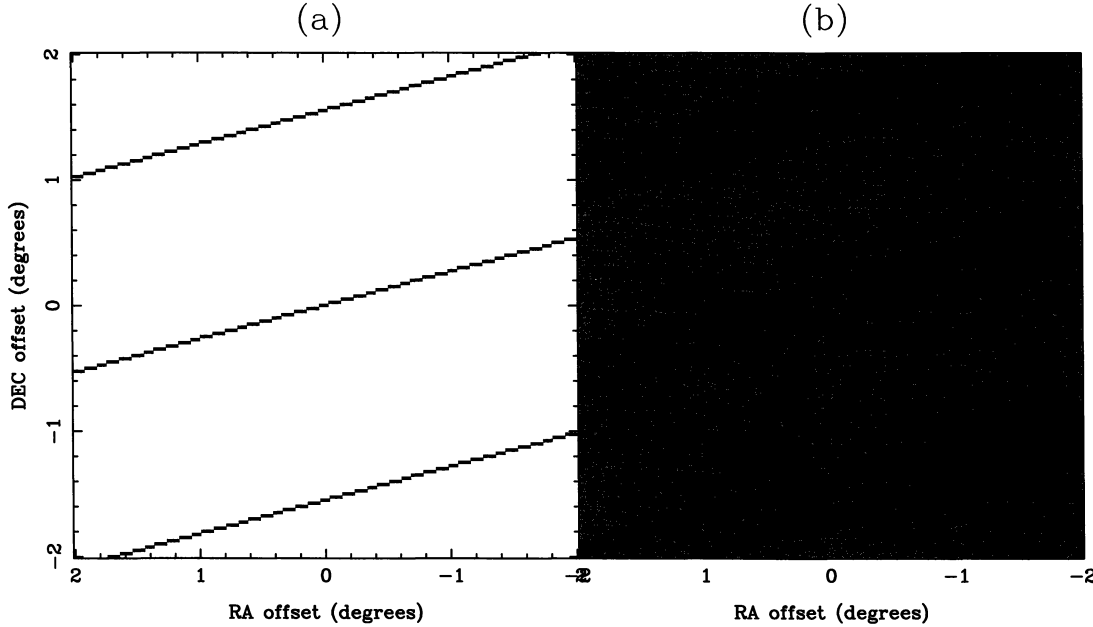


Figure 3—(a) Sampling function and (b) sensitivity pattern for a scanned multibeam observation. A rotation angle of 15° and a track separation of 93' is used. In (b), dark regions have higher than average sensitivity.

3 Beam Shapes and Observing Techniques

The theoretical beam patterns $B_i(\alpha, \delta)$ for each of the 13 beams have been added in quadrature as follows:

$$I_{13}(\alpha, \delta) = \sqrt{\sum_{i=1}^{13} B_i^2(\alpha, \delta)},$$

to give the beam sensitivity pattern shown in Figure 1. The feeds are spaced on a hexagonal grid of side 262.5 mm, which translates to an average beam separation on the sky of 29', or approximately 2 FWHP beamwidths. The outer beams are displaced by 51' from the central beam.

The overlap between the beams in Figure 1 is very small, and so a survey of a contiguous region of sky requires some method to fill in the gaps.

3.1 Point-and-shoot

The first method of interleaving the beams is perhaps most familiar to spectral-line radio astronomers, especially those used to the 'on-off' or position-switching observing technique. The 'point-and-shoot' method (also known as the 'hop-and-dwell' or 'step-and-stare' method) involves moving the telescope to the desired celestial position, integrating for a given time then moving to a new position to fill in the sensitivity gaps. We consider three methods to fill in these gaps, each with an increasing number of interleave positions.

The simplest method is to fill in the largest gaps in the beam pattern, which requires a total of three interleaved observations for each field. The optimum sky sampling function $S(\alpha, \delta)$ required to achieve this is shown in Figure 2 ($i = 3$), and the final sensitivity function, produced by convolving the sampling function with the beam sensitivity pattern,

$$I_0(\alpha, \delta) = \sqrt{S(\alpha, \delta) * I_{13}^2(\alpha, \delta)},$$

is also shown in Figure 2. The beams are unfortunately too far apart for this to be a useful mode of observing. The theoretical peak-to-peak sensitivity variation across the sky is a factor of 2.71 (Table 2).

Table 2. Uniformity of sensitivity and beam response for different spatial sampling functions

The observing method is point-and-shoot (pointed); i is the number of interleaved pointings per field (i.e. $i = 1$ gives the beam response of Figure 1); $\Delta\theta$ is the final beam separation on the sky; R_B is the ratio of the maximum and minimum beam response when all beams are linearly summed; R_S is the sensitivity variation, or the ratio of the maximum rms noise to the minimum rms expected in a survey of an extended region

Method	i	$\Delta\theta$	R_B	R_S
Pointed	1	28.6'	65	174
Pointed	3	16.2'	1.68	2.71
Pointed	4	14.0'	1.33	1.82
Pointed	16	7.0'	1.26	1.28

Variance of Image Sensitivity

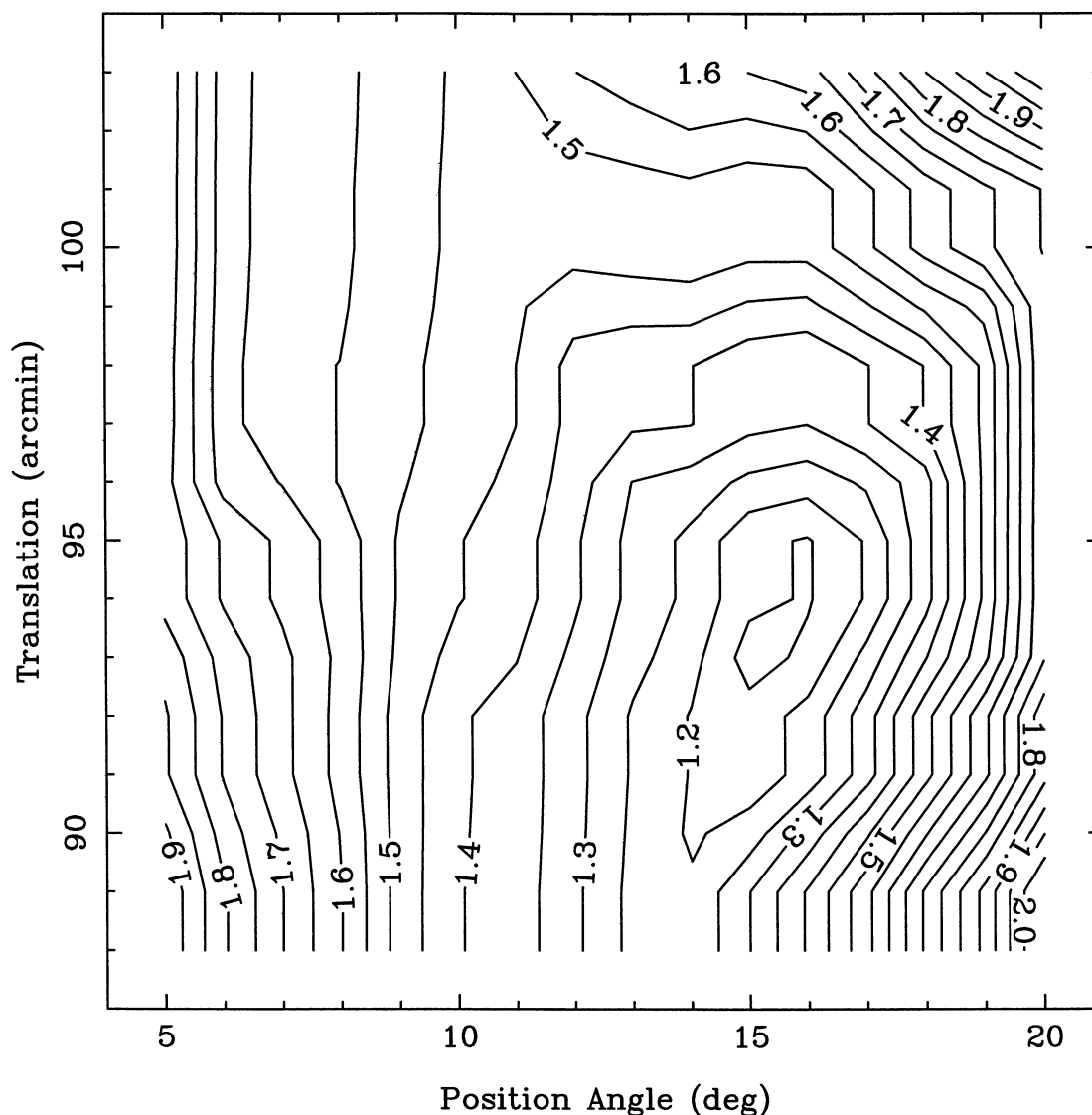


Figure 4—Contours of equal peak-to-peak sensitivity variation for images made by scanning the multibeam receiver at various position angles, and with various translations. The contour values are shown, and reach a minimum value of about 1.13 at $pa = 15^\circ$, translation = $93'$. The translation direction is taken to be along the vertical axis in Figure 3.

A second, more useful, sampling function is the diamond-shaped interleave shown in Figure 2 ($i = 4$), which puts extra beams at the midway position of the line joining each adjacent pair of beams. This gives an average beam separation of $14.0'$, which is slightly less than the theoretical FWHP beamwidth of $14.4'$. The resultant sensitivity variation for a survey of a large region of sky is 1.82 (Table 2).

The final discrete sampling function we consider is the nested diamond-in-diamond interleave pattern

of Figure 2 ($i = 16$). This achieves a somewhat better sensitivity variation of 1.28 (Table 2). More importantly, this sampling function provides a $7.0'$ beam separation which is comfortably close to the Nyquist separation for a hexagonal grid, which is $\lambda/(\sqrt{3}D) = 6.8'$ for $\lambda = 0.219$ m (1370 MHz).

3.2 Scanning

Scanning the telescope across the sky while observing is commonly used for continuum surveys in order to

reduce the effect of gain instabilities. An example is the Parkes–MIT–NRAO survey at 5 GHz (Griffith et al. 1994). With the Parkes multibeam array, scanning is also possible without substantial beam smearing.

Scans along horizontal or vertical tracks in Figure 1 will produce a ‘striped’ sensitivity function. However, scans at intermediate rotation angles can produce very uniform sensitivity distributions and Nyquist sampling. Based on the theoretical beam pattern, the fastest sampling function (in the sense of covering the most sky for the lowest number of scans) that gives uniform coverage and Nyquist sampling appears to be one based on an array rotation of 15° and an array translation of $93'$ as shown in Figure 3a. The sensitivity variation of such a scanning scheme (Figure 3b) is a very low 1.13. This is very acceptable, especially given that the efficiency ratio of the inner and outer beams is ~ 1.16 . The effect on sensitivity variation of nearby values of array rotation and translation is shown in Figure 4. Uniformity falls off very rapidly for rotations and translations much different from the values at the minimum. However, many other solutions exist which give extremely uniform sky coverage. These exist mainly at translations less than $35'$ and position angles in the range 7° to 15° , where there is much redundancy in sky coverage.

4 Overheads and Data Collection

For scans, the main constraint on the telescope scanning rate is the maximum rate at which the correlator can take data. For the HIPASS, it is expected that the smallest integration time of 5 s will be used. In order not to smear the $14.4'$ beam by more than 35%, a scan rate $< 1^\circ \text{ min}^{-1}$ is required. For all scans, apart from drift scans near the South Pole, many passes are required to build up the effective integration times listed in Table 1.

On the other hand, the point-and-shoot mode results in no beam-smearing but, as already mentioned, may involve significant telescope overheads. The existing Parkes control system has a delay of around 20 s even for short drives. Although this may soon change, such an overhead implies an unacceptable loss of observing time for integrations of around 2 min or less. Very long observations in point-and-shoot mode require ‘parallactification’ because of the alt–az nature of the Parkes telescope. However, it is important to note that changing parallactic angles during an observation, or between a ‘source’ and a ‘reference’ position, may adversely affect baseline stability because of subtle changes in the standing-wave characteristics of the telescope.

In both cases (scanning and point-and-shoot), collecting data every 5 s is advantageous for the suppression of time-variable interference (HIPASS’s greatest enemy). However, this creates a large volume of data (~ 0.5 TB for the whole survey). It is therefore important to have an automated data pipeline with as much processing performed online as is practical. Such a pipeline is being written using aips++.

Acknowledgments

Thanks to Trevor Bird for providing the theoretical model for the individual beam shapes used in this paper.

- Disney, M. J., & Banks, G. 1997, *PASA*, 14, 69
 Fisher, J. R. 1997, *PASA*, 14, 96
 Griffith, M. R., Wright, A. E., Burke, B. F., & Ekers, R. D. 1994, *ApJS*, 90, 179
 Johansson, J. F. 1995, in *Multi-Feed Systems for Radio Telescopes*, ASP Conf. Ser. 75, ed. D. T. Emerson & J. M. Payne (San Francisco: ASP), p. 34
 Ruze, J. 1965, *IEEE Trans. Antennas & Propagation*, 13, 660
 Schneider, S. E. 1997, *PASA*, 14, 99
 Staveley-Smith, L. et al. 1996, *PASA*, 13, 243